

PREPARED FOR SUBMISSION TO JHEP

Constraining Millicharged dark matter with Gravitational positivity bounds

Suro Kim, Pyungwon Ko

Korea Institute for Advanced Study, Seoul 02455, Republic of Korea

E-mail: surokim@kias.re.kr, pko@kias.re.kr

ABSTRACT: Gravitational positivity bounds provide consistency conditions for effective field theories with gravity. They turn out to be phenomenologically useful by providing lower bounds in parameters of new physics beyond the Standard Models (BSM). In this paper, we derive constraints on millicharged fermion dark matter models with massless dark photon using gravitational positivity bounds. Combining them with upper bounds from cosmological and astrophysical observations, we can severely constrain the parameter space of the model. In particular, we show that when the dark matter mass is lighter than the solar core temperature, most of the parameter region is excluded by combining gravitational positivity bounds and the stellar bounds.

Contents

1	Introduction	1
2	Millicharged Dark Matter	2
2.1	Milli-charged Dark Matter Model	2
2.2	Scattering amplitudes	3
3	Brief Review on Gravitational Positivity Bounds	5
4	Gravitational positivity bounds on millicharged DM	7
4.1	Constraints from $\gamma'\gamma' \rightarrow \gamma'\gamma'$ scattering	7
4.2	Constraints from $\gamma\gamma' \rightarrow \gamma\gamma'$ scattering	8
5	Conclusion	10

1 Introduction

Dark matter (DM) is now the universal paradigm supported by various cosmological and astrophysical observations based on gravitational interaction. However, its extremely tiny interaction with the standard model (SM) particles makes it difficult to detect directly in a non-gravitational manner. The worst possibility is that DM interacts with the SM sector only through gravitational interactions, meaning “*the dark matter is totally dark*”.

Considering that the standard model sector consists of many stable or long lived particles, it is rather unnatural to consider a single particle as DM compared to a dark sector. The most straightforward possibility as a dark sector would be DM which is charged under the hidden, unbroken $U(1)$ gauge symmetry. In this case, the dark photon γ' is massless and it can have interactions with the SM sector through a small kinetic mixing. Then, DM will have a tiny interaction with the SM sector and have a tiny electromagnetic charge as well. Such a dark matter model is called as a millicharged DM and has been studied extensively [1–29].

As a complementary method to experimental observations, it has been studied to find out consistency conditions for a UV completion of new physics. One of the well-established conditions is the positivity constraints on scattering amplitudes [30–35], see a review article [36], and their phenomenological applications [37–49]. Recently, this line of strategy has been extended by incorporating gravity effects to the positivity constraints [50–60] and applying them to various phenomenologies [61–66].

Let us comment on a few interesting points in phenomenological applications of the gravitational positivity bounds. First of all, constraints on renormalizable couplings can

be obtained through the positivity constraints on loop-level scattering amplitudes, whereas the ordinary positivity bounds usually gives constraints on couplings whose mass dimension is equal or larger than 8. The second point is that we can obtain lower bounds on couplings from gravitational positivity bounds. By combining the constraints from the gravitational positivity bounds with phenomenological upper bounds from observations, we can constrain a broad range of parameter spaces and can even exclude entire parameter space in some models. One example is the application on the massive dark photon. In Refs. [64, 66], the lower bound on the kinetic mixing between the photon and dark photon is obtained, which can be interpreted as “*the dark photon cannot be too dark*”. Also, most of the parameter region is excluded by combining the lower bounds from gravitational positivity bounds and phenomenological upper bounds from various observations. In this paper, we will elaborate on the gravitational positivity bounds in the millicharged DM models with a massless dark photon γ' coupled to massive fermion DM. γ' will couple to electrically charged particles of the SM through the $U(1)$ gauge kinetic mixing.

The organization of this paper is as follows. In Sec. 2 we will introduce the model for the millicharged DM and evaluate 1-loop amplitudes for $\gamma\gamma' \rightarrow \gamma\gamma'$ and $\gamma'\gamma' \rightarrow \gamma'\gamma'$ scatterings, where γ and γ' are the photon and the dark photon, respectively. Then, in Sec. 3 we will briefly review the gravitational positivity bounds. In Sec. 4, we will give constraints on parameters of the model using the gravitational positivity bounds and combine with phenomenological upper bounds obtained from various astrophysical and cosmological observations based, and then we will summarize.

2 Millicharged Dark Matter

2.1 Milli-charged Dark Matter Model

We first summarize the milli-charged dark matter model. We consider $U(1)_{\text{em}} \times U(1)_{\text{dark}}$, whose associated gauge fields are A_a and A_b , respectively. The action of the dark sector is given by

$$S_{\text{DS}} = \int d^4x \sqrt{-g} \left[-\frac{1}{4} F_{b,\mu\nu} F_b^{\mu\nu} - \frac{\varepsilon}{2} F_{a,\mu\nu} F_b^{\mu\nu} + \bar{\chi} (i\gamma^\mu \nabla_\mu + e' \gamma^\mu A_{b,\mu} - m) \chi \right]. \quad (2.1)$$

$F_{a,\mu\nu}$ and $F_{b,\mu\nu}$ are the field strength for each gauge boson. ε measures the $U(1)$ gauge kinetic mixing and we assume that $\varepsilon \ll 1$ throughout this paper. χ is a fermionic dark matter with the dark $U(1)_{\text{dark}}$ charge, e' , and mass, m . ∇ is the covariant derivative with the spin connection. Let us perform the following field redefinition and diagonalize kinetic terms as

$$\begin{aligned} \begin{pmatrix} A \\ A' \end{pmatrix} &= \frac{1}{\sqrt{2 - 2\sqrt{1 - \varepsilon^2}}} \begin{pmatrix} \varepsilon & 1 - \sqrt{1 - \varepsilon^2} \\ 1 - \sqrt{1 - \varepsilon^2} & \varepsilon \end{pmatrix} \begin{pmatrix} A_a \\ A_b \end{pmatrix} \\ &\approx \begin{pmatrix} 1 & \frac{\varepsilon}{2} \\ \frac{\varepsilon}{2} & 1 \end{pmatrix} \begin{pmatrix} A_a \\ A_b \end{pmatrix} + \mathcal{O}(\varepsilon^2). \end{aligned} \quad (2.2)$$

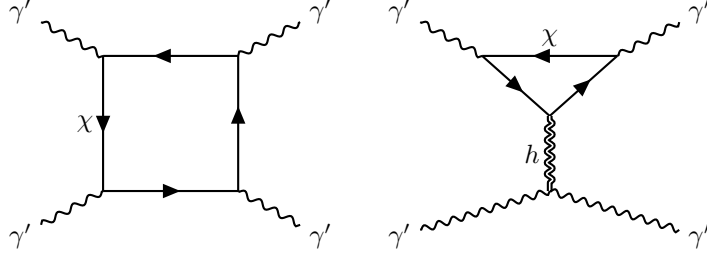


Figure 1. Feynman diagrams for $\gamma'\gamma' \rightarrow \gamma'\gamma'$.

We call A and A' photon and dark photon, respectively. Note that the diagonalization generates tiny couplings between the photon and dark matter χ , thereby motivating the “milli-charged DM model”:

$$S_{\text{DS}} \approx \int d^4x \sqrt{-g} \left[-\frac{1}{4} F'_{\mu\nu} F'^{\mu\nu} + \bar{\chi} \left(i\gamma^\mu \nabla_\mu + e' \gamma^\mu A'_\mu - \frac{\varepsilon}{2} e' \gamma^\mu A_\mu - m \right) \chi + \mathcal{O}(\epsilon^2) \right]. \quad (2.3)$$

In a similar manner, it generates tiny coupling between the dark photon and the electrically charged standard model particles by $S_{\text{SM}}|_{A \rightarrow A - \varepsilon A' / 2}$. In the next subsection, we will analyze $\gamma'\gamma' \rightarrow \gamma'\gamma'$ and $\gamma\gamma' \rightarrow \gamma\gamma'$ scatterings through the loops involving DM fermions and electrically charged SM particles.

2.2 Scattering amplitudes

Let us define the following helicity combinations of the scattering amplitudes for $\gamma'\gamma' \rightarrow \gamma'\gamma'$ and $\gamma\gamma' \rightarrow \gamma\gamma'$:

$$\mathcal{M} = \frac{1}{4} [\mathcal{M}(1^+ 2^+ 3^+ 4^+) + \mathcal{M}(1^+ 2^- 3^+ 4^-) + \mathcal{M}(1^- 2^+ 3^- 4^+) + \mathcal{M}(1^- 2^- 3^- 4^-)]. \quad (2.4)$$

The superscript \pm represents the helicity of each external particle. Note that we only have transverse modes because both photon and dark photon are massless in our model.

Let us first evaluate $\gamma'\gamma' \rightarrow \gamma'\gamma'$. We use the Mathematica packages FEYNARTS [67] and FEYNCALC [68], to calculate the one-loop diagrams and PACKAGE-X [69] to evaluate the loop integrals. The leading non-gravitational contribution comes from the dark matter loop (the left figure in Fig. 1), which is given by

$$\begin{aligned} \mathcal{M}_{\text{QED}'} = & -\frac{2\alpha'^2}{s^2} \left[2\sqrt{s(s-4m^2)}(s+4m^2) \log \left(\frac{\sqrt{s(s-4m^2)} + 2m^2 - s}{2m^2} \right) \right. \\ & \left. + (s^2 + 4m^2s - 8m^4) \log^2 \left(\frac{\sqrt{s(s-4m^2)} + 2m^2 - s}{2m^2} \right) + 6s^2 \right] \\ & + (s \leftrightarrow -s) + \mathcal{O}(t). \end{aligned} \quad (2.5)$$

where $\alpha' = e'^2/4\pi$. We expanded the amplitude around $t = 0$ for later convenience.

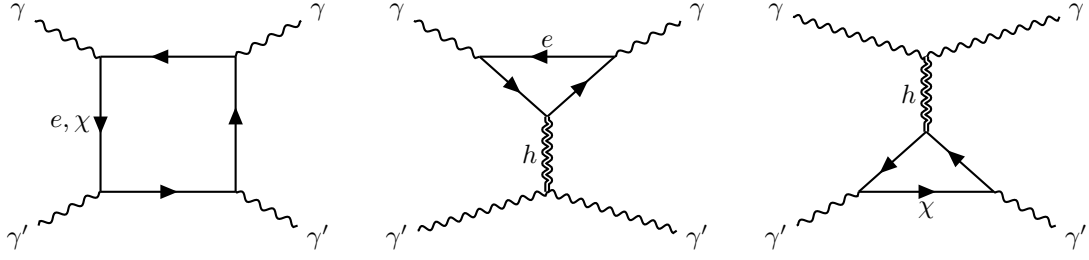


Figure 2. Feynman diagrams for $\gamma\gamma' \rightarrow \gamma\gamma'$ mediated by the electron and the dark matter.

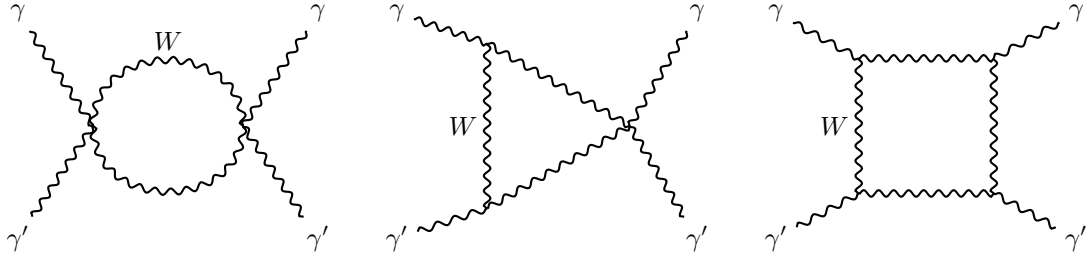


Figure 3. Feynman diagrams for $\gamma\gamma' \rightarrow \gamma\gamma'$, mediated by W boson.

On the other hand, the contribution from the graviton exchange (the right figure in Fig. 1) is given by

$$\begin{aligned} \mathcal{M}_{\text{GR}} = & -\frac{\alpha'}{360\pi m^2 M_{\text{Pl}}^2 s} \left[120m^2 \sqrt{s(s-4m^2)}(s+5m^2) \log \left(\frac{\sqrt{s(s-4m^2)} + 2m^2 - s}{2m^2} \right) \right. \\ & + 180m^4(s+2m^2s) \log^2 \left(\frac{\sqrt{s(s-4m^2)} + 2m^2 - s}{2m^2} \right) \\ & \left. + s(11s^2 + 1560m^4) \right] + (s \leftrightarrow -s) + \mathcal{O}(t), \end{aligned} \quad (2.6)$$

in harmonic/de Donder gauge. Note that we have already performed the wave function renormalization of external dark photons.

Next, let us move on to $\gamma\gamma' \rightarrow \gamma\gamma'$ scattering. Without graviton exchange, we have contributions from DM, an electron, and a W boson loops.¹ The DM loop contribution has the same form as (2.5) with an additional factor $\epsilon^2/4$. It is straightforward to calculate the contribution from an electron loop (2.5), which is given by exchanging $m \rightarrow m_e$ and $\alpha' \rightarrow \alpha$ from the DM loops. In the electroweak sector, the leading contribution comes from

¹Here we keep the lightest charged fermion and boson loops only. Heavier particle contributions will be suppressed relative to these by calculable amounts based on Eqs. (4.4)-(4.6).

the W-boson loop (Fig. 3), which is given in unitary gauge by

$$\begin{aligned}\mathcal{M}_{\text{Weak}} = & \frac{\varepsilon^2 \alpha^2}{2m_W^2 s^2} \left[\sqrt{s(s-4m)} (4s^2 + 3m_W^2 s + 12m_W^4) \log \left(\frac{\sqrt{s(s-4m_W^2)} + 2m_W^2 - s}{2m_W^2} \right) \right. \\ & + 6m_W^4 (s - 2m_W^2) \log^2 \left(\frac{\sqrt{s(s-4m_W^2)} + 2m_W^2 - s}{2m_W^2} \right) + 9m_W^2 s^2 \Big] \\ & + (s \leftrightarrow -s) + \mathcal{O}(t),\end{aligned}\tag{2.7}$$

around $t = 0$. The gravitational contribution to the $\gamma\gamma' \rightarrow \gamma\gamma'$ scattering around $t = 0$ (the middle and the right Feynman diagrams of Fig. 2) is given by

$$\mathcal{M}_{\text{GR}} = -\frac{11\alpha s^2}{360\pi m_e^2 M_{\text{Pl}}^2} - \frac{11\alpha' s^2}{360\pi m^2 M_{\text{Pl}}^2} + \mathcal{O}(t),\tag{2.8}$$

after wave function renormalization of external particles.

3 Brief Review on Gravitational Positivity Bounds

In this section, we introduce observables which we will calculate in the next section and the consequences from the gravitational positivity bounds. Throughout this paper, we will follow the notation and the workflow well established in [66].

Let $\mathcal{M}(s, t)$ be the s - u symmetric scattering amplitude for $AB \rightarrow AB$, where s , t , and u are the Mandelstam variables. We assume the following properties for \mathcal{M} .

1. Analyticity: On the physical sheets of complex s -plane, $\mathcal{M}(s, t \rightarrow -0)$ is analytic, excluding poles and branch cuts on the real axis of s , which correspond to the on-shell tree-level and loop contributions to \mathcal{M} , respectively.
2. Unitarity: The imaginary part of \mathcal{M} is non-negative.
3. Mild behavior at UV: \mathcal{M} is bounded by s^2 in the high energy,

$$\lim_{|s| \rightarrow \infty} \frac{\mathcal{M}(s, t \rightarrow -0)}{s^2} = 0.\tag{3.1}$$

Let us elaborate more on the last assumption. In the absence of gravity, it is guaranteed in local QFTs by the Froissart-Martin bound [70–72]. On the other hand, it has some subtleties when we incorporate gravity into the discussion. Scattering amplitudes for graviton exchanges in the t -channel include terms such as $\sim -s^2/(M_{\text{Pl}}^2 t)$, which breaks the third assumption for the fixed negative t . To address the issue, in [54] the authors suggested to assume the Regge behavior of high energy scatterings:

$$\lim_{|s| \rightarrow \infty} \text{Im} \mathcal{M}(s, t) \approx f(t) \left(\frac{\alpha' s}{4} \right)^{2+j(t)},\tag{3.2}$$

which is realized in a weakly coupled UV completion of gravity. $j(t)$ is negative for fixed negative t so that it satisfies the third assumption. α' is the scale of Reggeization. Having such cases in mind, we will assume that the third condition holds, even though we will not specify the UV theory throughout this paper.

Next, we briefly review what the gravitational positivity bounds states.² In this paper, we focus on the case that the external particles are all massless so that $s + t + u = 0$. We expand \mathcal{M} in terms of the Mandelstam variables in the low energy limit. Let a_2 be an s^2 coefficient of a scattering amplitude after subtracting the graviton t -channel pole;

$$a_2 := \lim_{t \rightarrow -0} \left[\frac{\partial^2 \mathcal{M}(s, t)}{\partial s^2} + \frac{2}{M_{\text{Pl}}^2 t} \right]_{s=0}. \quad (3.3)$$

The first term can be rewritten by picking up the residue at the origin ($s = 0$),

$$a_2 = \lim_{t \rightarrow -0} \left[\frac{1}{\pi i} \oint ds \frac{\mathcal{M}(s, t)}{s^3} + \frac{2}{M_{\text{Pl}}^2 t} \right]_{s=0}. \quad (3.4)$$

From the assumption 1 and 3, we can justify the following deformation of the integration contour for the first term,

$$a_2 = \lim_{t \rightarrow -0} \left[\frac{4}{\pi} \int_{m_{\text{th}}^2}^{\infty} ds \frac{\text{Im} \mathcal{M}(s, t)}{s^3} + \frac{2}{M_{\text{Pl}}^2 t} \right]_{s=0}, \quad (3.5)$$

where m_{th} is the mass of the lightest intermediate state. In our case, $m_{\text{th}}^2 = 4m_e^2$ when $m_e < m$ or $m_{\text{th}}^2 = 4m^2$ when $m < m_e$. Next, we introduce the reference scale of the theory, Λ , below which we assume our EFT is valid. Below Λ , \mathcal{M} is calculable quantity within our framework, then we can define $B(\Lambda)$ as a s^2 coefficient subtracting contributions below Λ :

$$B(\Lambda) := a_2 - \frac{4}{\pi} \int_{m_{\text{th}}^2}^{\Lambda^2} ds \frac{\text{Im} \mathcal{M}(s, t=0)}{s^3}. \quad (3.6)$$

The gravitational positivity bounds states that there exist the lower bound on $B(\Lambda)$ [54]

$$B(\Lambda) \geq \frac{\sigma}{M_{\text{Pl}}^2 M^2}, \quad (3.7)$$

The sign $\sigma = \pm 1$, and the scale M are determined by details of UV behaviors of scattering amplitudes, e.g. the Regge behavior. Throughout this paper, we will assume that M is larger than Λ , the electron mass m_e and a dark matter mass m . In this case, we can ignore the r.h.s of (3.7), then the bound is simplified as

$$B(\Lambda) \gtrsim 0. \quad (3.8)$$

Since we include the gravity in discussion, $B(\Lambda)$ contains both gravitational contributions $B_{\text{grav}}(\Lambda)$, and non-gravitational contributions $B_{\text{non-grav}}(\Lambda)$. Among them, $B_{\text{non-grav}}(\Lambda)$ give always positive contributions whereas $B_{\text{grav}}(\Lambda)$ might give negative contributions as we will see later. Therefore, non-gravitational contribution should compensate the gravitational contribution to satisfy the bound (3.8). Such behavior implies that the gravitational positivity bounds constrain renormalizable couplings, whereas the non-gravitational positivity bounds usually constrain nonrenormalizable couplings such as dimension-8 couplings.

²See [54] for the detailed derivation. Also refer to [66] for the guidelines for application to phenomenology.

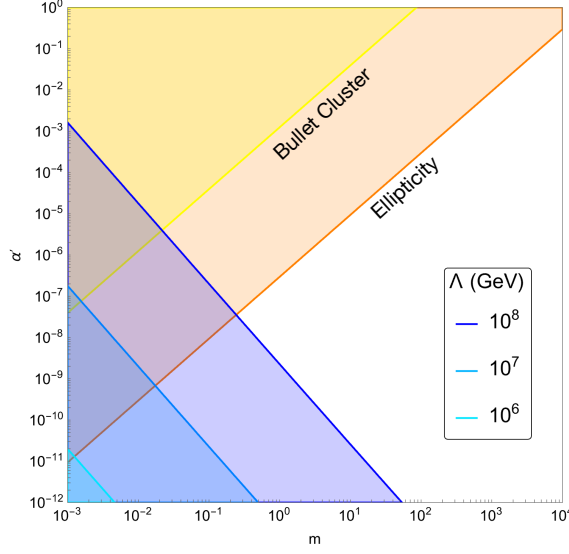


Figure 4. Constraints on m - α' plane from the gravitational positivity bounds and cosmological constraints. The blue regions are excluded by the gravitational positivity bounds for $\Lambda = 10^8, 10^7$, and 10^6 GeV, respectively. The orange region is constrained by ellipticity of galactic dark matter halos. The yellow region is constrained by the Bullet Cluster [14].

4 Gravitational positivity bounds on millicharged DM

In this section, we obtain the constraints from the gravitational positivity bounds on the millicharged DM model and compare with the phenomenological constraints from astrophysical and cosmological observations.

4.1 Constraints from $\gamma'\gamma' \rightarrow \gamma'\gamma'$ scattering

Let us start from the bound related to $\gamma'\gamma' \rightarrow \gamma'\gamma'$ scattering. To get a bound on the model parameters, α' , ε , and m , we evaluate $B(\Lambda)$ for each scattering amplitude. $B(\Lambda)$ for the dark matter loop and graviton exchange are given by

$$B_{\text{QED}'} \approx \frac{16\alpha'^2}{\Lambda^4} \left(\ln \frac{\Lambda}{m} - \frac{1}{4} \right), \quad (4.1)$$

$$B_{\text{GR}} \approx -\frac{11\alpha'}{90\pi m^2 M_{\text{Pl}}^2}, \quad (4.2)$$

where $\Lambda \gg m_e$. Note that the gravitational contribution is negative so that we can obtain non-trivial constraints. Since (4.2) is dominant over the r.h.s of (3.7) when $M \gg m/e'$, we can use (3.8). As a result, we obtain the following lower bound on α' :

$$\alpha' \left(\ln \frac{\Lambda}{m} - \frac{1}{4} \right) > \frac{11}{1440\pi} \left(\frac{\Lambda}{m} \right)^2 \left(\frac{\Lambda}{M_{\text{Pl}}} \right)^2. \quad (4.3)$$

This bound is plotted in Fig. 4 with the corresponding cosmological and astrophysical constraints [14]. The DM self-interaction mediated by the dark photon is constrained by

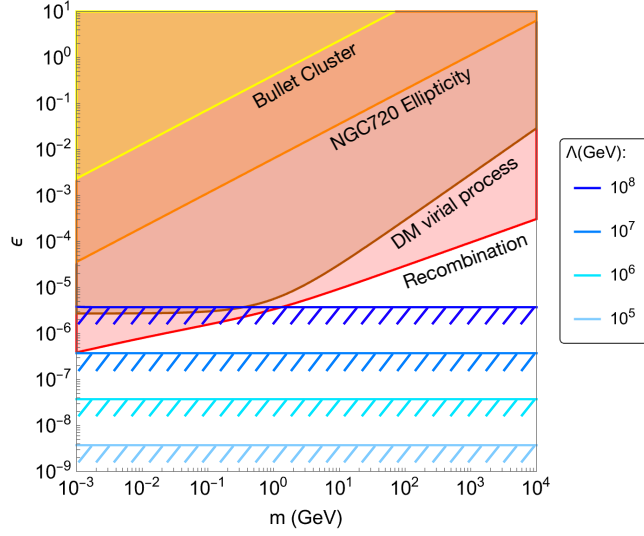


Figure 5. Constraints on m - ε plane from the gravitational positivity bounds and cosmological constraints. Here we substituted the smallest value for α' from Eq. (4.3). The regions below the each blue lines are excluded by the gravitational positivity bounds for $\Lambda = 10^8, 10^7, 10^6$, and 10^5 GeV, respectively. The red, brown, orange, and yellow regions are constrained by decoupling before the recombination era, dark matter virial process, of galactic dark matter halos, and the Bullet Cluster, respectively.

the Bullet Cluster and an ellipticity of galactic dark matter halos, as illustrated with the yellow and orange region, respectively. Note that that the higher Λ leads to the stronger gravitational positivity bounds.

One can check that in the case of the light dark matter, $m \sim 10^{-3}$ GeV and when $\Lambda \gtrsim 10^6$ GeV, the whole region of α' is excluded by combining the cosmological and astrophysical constraints and the gravitational positivity bounds. On the other hand, when the dark matter mass becomes larger, both constraints become weaker and a broad region is allowed.

4.2 Constraints from $\gamma\gamma' \rightarrow \gamma\gamma'$ scattering

Next, we move on to the bounds from $\gamma\gamma' \rightarrow \gamma\gamma'$ scattering. We have three contributions from the box diagrams with dark matter and electron loops, W boson loops, and graviton exchange, whose $B(\Lambda)$ are respectively given by

$$B_{e,\chi} \approx \frac{4\varepsilon^2}{\Lambda^4} \left[\alpha^2 \left(\ln \frac{\Lambda}{M_e} - \frac{1}{4} \right) + \alpha'^2 \left(\ln \frac{\Lambda}{m} - \frac{1}{4} \right) \right]. \quad (4.4)$$

$$B_{\text{Weak}} \approx \frac{8\varepsilon^2\alpha^2}{m_W^2\Lambda^2}. \quad (4.5)$$

$$B_{\text{GR}} \approx -\frac{11\alpha}{180\pi m_e^2 M_{\text{Pl}}^2} - \frac{11\alpha'}{180\pi m^2 M_{\text{Pl}}^2}, \quad (4.6)$$

where we take $\Lambda \gg m, m_e, m_W$.

Similarly to the previous subsection, when $M \gg m_e/e$, m/e' , the r.h.s of (3.7) can be ignored so that we can use (3.8) to derive the following bounds:

$$\begin{aligned} \varepsilon^2 \left[\alpha^2 \left(\ln \frac{\Lambda}{m_e} - \frac{1}{4} + 2 \left(\frac{\Lambda^2}{m_W^2} \right)^2 \right) + \alpha'^2 \left(\ln \frac{\Lambda}{m} - \frac{1}{4} \right) \right] \\ > \frac{11\alpha}{720\pi} \left(\frac{\Lambda}{M_{\text{Pl}}} \right)^2 \left(\frac{\Lambda}{M_e} \right)^2 \left[1 + \frac{\alpha'}{\alpha} \left(\frac{m_e}{m} \right)^2 \right]. \end{aligned} \quad (4.7)$$

Let us first focus on the WIMP mass range, $10^{-3} \text{ GeV} \lesssim m \lesssim 10^4 \text{ GeV}$. See Fig. 5 for the positivity bounds and cosmological and astrophysical constraints in the $m - \varepsilon$ plane. Note that kinetic mixing ε generates DM couplings to SM sector, that gives following cosmological constraints [15]. DM should decouple from the SM sector before recombination, not to affect to the CMB data, whose bound on ε is depicted by the red region in Fig. 5. On top of that, if DM couples too strongly to the SM sector after recombination, the SM sector transfers energy to DM and it modifies the DM virialization process, whose bound is shown as the brown region in Fig. 5. On the other hand, ε also generates the DM self-interaction through the photon exchange. It gives constraints from the Bullet cluster and ellipticity of galactic dark matter halos, same as the case of α' , which are shown as the yellow and orange region in Fig. 5, respectively.

Next, we move on to the lighter dark matter case, whose mass is lighter than the solar core temperature, $T_\odot \sim 1 \text{ keV}$. In this mass region, there exist various phenomena such as dark solar wind [73]. The most relevant cosmological constraint for this case comes from the stellar bound, which states that the coupling between a light dark matter and the SM particles should be small enough to avoid a pair creation of DM from the SM plasma inside the Sun and anomalous evolution in red giants. The most stringent stellar bound is given by [16]

$$\varepsilon \alpha'^{1/2} \lesssim 2 \times 10^{-15}. \quad (4.8)$$

See Fig. 6 for the constraints on $\varepsilon - \alpha'$ plane. In the left panel, we fixed $\Lambda = 1 \text{ TeV}$ and varied m , whereas on the right panel we fixed $m = 10^{-6} \text{ GeV}$ and varied Λ . We took $\Lambda \gtrsim 1 \text{ TeV}$, assuming no dark particles coupled to the photon are found below 1 TeV.

Note that the larger Λ and the lower m , the stronger bound from gravitational positivity. The behavior of blue lines in Fig. 6 can be understood as follows. When $\alpha \lesssim \alpha'$, the second terms of each side of (4.7) is dominant, so that it generates a slope like $\alpha' \propto \varepsilon^{-2}$. On the other hand, when $\alpha(m/m_e)^2 \lesssim \alpha' \lesssim \alpha$, the first term on the L.H.S becomes dominant, then the slope changes as $\alpha' \propto \varepsilon^2$. Finally, when $\alpha' \lesssim \alpha(m/m_e)^2$, the first term on the R.H.S becomes dominant so that it draws a vertical lines. By combining the stellar bound and the gravitational positivity bounds, we obtain the stringent bounds³: $\alpha' \lesssim 2.6 \times 10^{-10}$ and $\varepsilon \gtrsim 3.6 \times 10^{-11}$, when $\Lambda = 1 \text{ TeV}$.

³In [74], a qualitatively similar bound is obtained from the other consistency condition with quantum gravity, the weak gravity conjecture. Nevertheless, our analysis yields a quantitatively stronger bound.

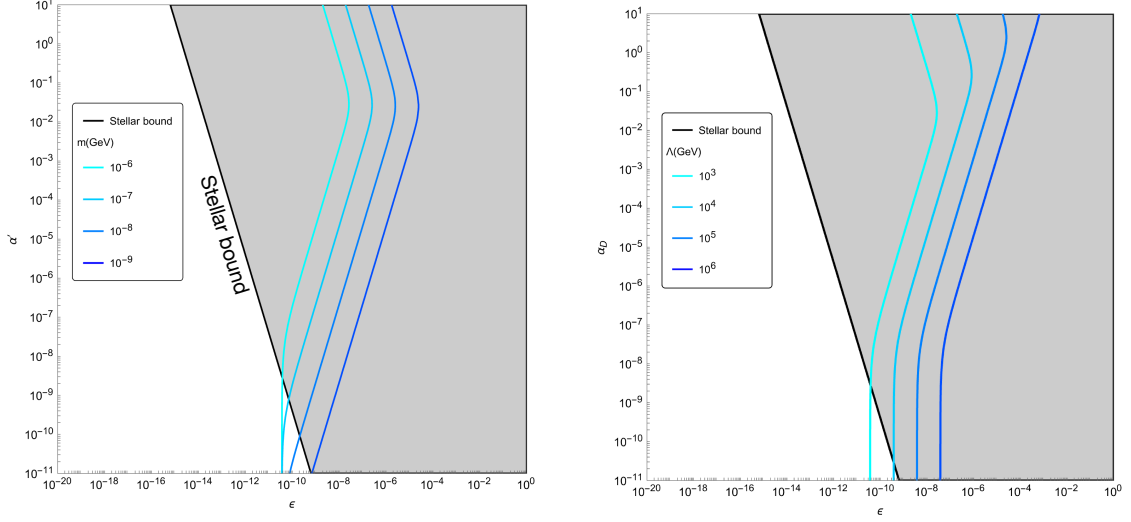


Figure 6. The constraints on ε - α' plane from the gravitational positivity bounds and the stellar bound. The shaded region is forbidden by the stellar bound. The left region of each blue line is excluded. In the left plot, we fixed the reference scale Λ and vary DM mass m , whereas in the right plot we fixed m and vary Λ . (Left) Each blue lines are for $m = 10^{-6}, 10^{-7}, 10^{-8}$, and 10^{-9} GeV, where $\Lambda = 10^3$ GeV. (Right) Each blue lines are for $\Lambda = 10^3, 10^4, 10^5$, and 10^6 GeV, where $m = 10^{-6}$ GeV.

5 Conclusion

In this paper, we discussed the application of the gravitational positivity bounds on the millicharged dark matter model and obtained constraints on the model parameters α' , ε , and m . In particular, in the case that the dark matter mass is below the solar core temperature $T_\odot \sim 1$ keV, we obtained the stringent bounds, $\alpha' \lesssim 2.6 \times 10^{-10}$ and $\varepsilon \gtrsim 3.6 \times 10^{-11}$ (See Fig. 6).

In the case of the WIMP mass range, we obtained the relatively relaxed bound, which is plotted in Fig. 4 and Fig. 5. When the dark matter mass is light, $m \sim 10^{-3}$ GeV, and for $\Lambda > 10^7$ GeV, all the region of α' and ε is excluded by combining the cosmological constraints and the gravitational positivity bounds.

Although the gravitational positivity bounds are effective to give constraints on the millicharged dark matter model, it has limitations. The dark photon can have a kinetic mixing to the standard model gauge bosons, which leads to mixings to other standard model particles, such as the QCD sector. For example, the dark photon can have a coupling with vector mesons through the kinetic mixing with photon. Then, in the forward limit the $\gamma\gamma' \rightarrow \gamma\gamma'$ scattering includes the non-perturbative effects such as exchanges of the Reggeon or the Pomeron at high energy. They possibly give a large non-gravitational contribution to the scattering amplitudes at high energy and then may significantly modify the constraints which are obtained in this paper.

Note that the gravitational positivity bounds are applicable to various dark matter

models. In particular, they can be highly advantageous for scenarios wherein observational data stringently restrict the parameter space. An immediate example would be non-Abelian dark gauge models, in which interactions between dark matter and dark radiation can affect the matter power spectrum and σ_8 , as well as dark radiation itself can change the Hubble parameter H_0 [75, 76]. The gauge coupling should be very tiny so that the matter power spectrum is not suppressed too much. Investigating whether the phenomenologically acceptable dark gauge coupling satisfies the gravitational positivity bounds would be interesting. We leave such discussions for future works.

Acknowledgments

We draw Feynman diagrams using the Mathematica package TikZ-Feynman [77]. This work is supported in part by KIAS Individual Grants under Grant No. PG082102 (S.K.), and No. PG021403 (P.K.) at Korea Institute for Advanced Study.

References

- [1] B. Holdom, *Two $U(1)$'s and Epsilon Charge Shifts*, Phys. Lett. B **166** (1986) 196–198.
- [2] H. Goldberg and L. J. Hall, *A New Candidate for Dark Matter*, Phys. Lett. B **174** (1986) 151.
- [3] A. De Rujula, S. L. Glashow and U. Sarid, *CHARGED DARK MATTER*, Nucl. Phys. B **333** (1990) 173–194.
- [4] D. E. Brahm and L. J. Hall, *$U(1)$ -prime DARK MATTER*, Phys. Rev. D **41** (1990) 1067.
- [5] S. Dimopoulos, D. Eichler, R. Esmailzadeh and G. D. Starkman, *Getting a Charge Out of Dark Matter*, Phys. Rev. D **41** (1990) 2388.
- [6] S. Davidson and M. E. Peskin, *Astrophysical bounds on millicharged particles in models with a paraphoton*, Phys. Rev. D **49** (1994) 2114–2117 [[hep-ph/9310288](#)].
- [7] S. Davidson, S. Hannestad and G. Raffelt, *Updated bounds on millicharged particles*, JHEP **05** (2000) 003 [[hep-ph/0001179](#)].
- [8] S. L. Dubovsky, D. S. Gorbunov and G. I. Rubtsov, *Narrowing the window for millicharged particles by CMB anisotropy*, JETP Lett. **79** (2004) 1–5 [[hep-ph/0311189](#)].
- [9] L. Ackerman, M. R. Buckley, S. M. Carroll and M. Kamionkowski, *Dark Matter and Dark Radiation*, Phys. Rev. D **79** (2009) 023519 [[0810.5126](#)].
- [10] L. Chuzhoy and E. W. Kolb, *Reopening the window on charged dark matter*, JCAP **07** (2009) 014 [[0809.0436](#)].
- [11] J. L. Feng, H. Tu and H.-B. Yu, *Thermal Relics in Hidden Sectors*, JCAP **10** (2008) 043 [[0808.2318](#)].
- [12] S. Gardner and D. C. Latimer, *Dark Matter Constraints from a Cosmic Index of Refraction*, Phys. Rev. D **82** (2010) 063506 [[0904.1612](#)].
- [13] D.-C. Dai, K. Freese and D. Stojkovic, *Constraints on dark matter particles charged under a hidden gauge group from primordial black holes*, JCAP **06** (2009) 023 [[0904.3331](#)].

- [14] J. L. Feng, M. Kaplinghat, H. Tu and H.-B. Yu, *Hidden Charged Dark Matter*, JCAP **07** (2009) 004 [[0905.3039](#)].
- [15] S. D. McDermott, H.-B. Yu and K. M. Zurek, *Turning off the Lights: How Dark is Dark Matter?*, Phys. Rev. D **83** (2011) 063509 [[1011.2907](#)].
- [16] H. Vogel and J. Redondo, *Dark Radiation constraints on minicharged particles in models with a hidden photon*, JCAP **02** (2014) 029 [[1311.2600](#)].
- [17] G. Shiu, P. Soler and F. Ye, *Milli-Charged Dark Matter in Quantum Gravity and String Theory*, Phys. Rev. Lett. **110** (2013), no. 24, 241304 [[1302.5471](#)].
- [18] A. Haas, C. S. Hill, E. Izaguirre and I. Yavin, *Looking for milli-charged particles with a new experiment at the LHC*, Phys. Lett. B **746** (2015) 117–120 [[1410.6816](#)].
- [19] D. Ejlli, *Millicharged fermion vacuum polarization in a cosmic magnetic field and generation of CMB elliptic polarization*, Phys. Rev. D **96** (2017), no. 2, 023540 [[1704.01894](#)].
- [20] A. Berlin, N. Blinov, G. Krnjaic, P. Schuster and N. Toro, *Dark Matter, Millicharges, Axion and Scalar Particles, Gauge Bosons, and Other New Physics with LDMX*, Phys. Rev. D **99** (2019), no. 7, 075001 [[1807.01730](#)].
- [21] S. N. Gninenko, D. V. Kirpichnikov and N. V. Krasnikov, *Probing millicharged particles with NA64 experiment at CERN*, Phys. Rev. D **100** (2019), no. 3, 035003 [[1810.06856](#)].
- [22] K. J. Kelly and Y.-D. Tsai, *Proton fixed-target scintillation experiment to search for millicharged dark matter*, Phys. Rev. D **100** (2019), no. 1, 015043 [[1812.03998](#)].
- [23] R. Harnik, Z. Liu and O. Palamara, *Millicharged Particles in Liquid Argon Neutrino Experiments*, JHEP **07** (2019) 170 [[1902.03246](#)].
- [24] J. Liang, Z. Liu, Y. Ma and Y. Zhang, *Millicharged particles at electron colliders*, Phys. Rev. D **102** (2020), no. 1, 015002 [[1909.06847](#)].
- [25] S. Foroughi-Abari, F. Kling and Y.-D. Tsai, *Looking forward to millicharged dark sectors at the LHC*, Phys. Rev. D **104** (2021), no. 3, 035014 [[2010.07941](#)].
- [26] D. Budker, P. W. Graham, H. Ramani, F. Schmidt-Kaler, C. Smorra and S. Ulmer, *Millicharged Dark Matter Detection with Ion Traps*, PRX Quantum **3** (2022), no. 1, 010330 [[2108.05283](#)].
- [27] A. Berlin, R. Tito D’Agnolo, S. A. R. Ellis and J. I. Radkovski, *Signals of millicharged dark matter in light-shining-through-wall experiments*, JHEP **08** (2023) 017 [[2305.05684](#)].
- [28] A. Hebecker, J. Jaeckel and R. Kuespert, *Small Kinetic Mixing in String Theory*, [2311.10817](#).
- [29] D. F. G. Fiorillo and E. Vitagliano, *Self-interacting dark sectors in supernovae are fluid*, [2404.07714](#).
- [30] T. N. Pham and T. N. Truong, *Evaluation of the Derivative Quartic Terms of the Meson Chiral Lagrangian From Forward Dispersion Relation*, Phys. Rev. D **31** (1985) 3027.
- [31] M. R. Pennington and J. Portoles, *The Chiral Lagrangian parameters, l_1 , l_2 , are determined by the rho resonance*, Phys. Lett. B **344** (1995) 399–406 [[hep-ph/9409426](#)].
- [32] B. Ananthanarayan, D. Toublan and G. Wanders, *Consistency of the chiral pion pion scattering amplitudes with axiomatic constraints*, Phys. Rev. D **51** (1995) 1093–1100 [[hep-ph/9410302](#)].

- [33] J. Comellas, J. I. Latorre and J. Taron, *Constraints on chiral perturbation theory parameters from QCD inequalities*, Phys. Lett. B **360** (1995) 109–116 [[hep-ph/9507258](#)].
- [34] A. Adams, N. Arkani-Hamed, S. Dubovsky, A. Nicolis and R. Rattazzi, *Causality, analyticity and an IR obstruction to UV completion*, JHEP **10** (2006) 014 [[hep-th/0602178](#)].
- [35] A. Adams, A. Jenkins and D. O’Connell, *Signs of analyticity in fermion scattering*, [0802.4081](#).
- [36] C. de Rham, S. Kundu, M. Reece, A. J. Tolley and S.-Y. Zhou, *Snowmass White Paper: UV Constraints on IR Physics*, in *Snowmass 2021*. 3, 2022. [2203.06805](#).
- [37] L. Vecchi, *Causal versus analytic constraints on anomalous quartic gauge couplings*, JHEP **11** (2007) 054 [[0704.1900](#)].
- [38] C. Zhang and S.-Y. Zhou, *Positivity bounds on vector boson scattering at the LHC*, Phys. Rev. D **100** (2019), no. 9, 095003 [[1808.00010](#)].
- [39] Q. Bi, C. Zhang and S.-Y. Zhou, *Positivity constraints on aQGC: carving out the physical parameter space*, JHEP **06** (2019) 137 [[1902.08977](#)].
- [40] G. N. Remmen and N. L. Rodd, *Consistency of the Standard Model Effective Field Theory*, JHEP **12** (2019) 032 [[1908.09845](#)].
- [41] S. Kim, T. Noumi, K. Takeuchi and S. Zhou, *Heavy Spinning Particles from Signs of Primordial Non-Gaussianities: Beyond the Positivity Bounds*, JHEP **12** (2019) 107 [[1906.11840](#)].
- [42] G. N. Remmen and N. L. Rodd, *Flavor Constraints from Unitarity and Analyticity*, Phys. Rev. Lett. **125** (2020), no. 8, 081601 [[2004.02885](#)], [Erratum: Phys.Rev.Lett. 127, 149901 (2021)].
- [43] K. Yamashita, C. Zhang and S.-Y. Zhou, *Elastic positivity vs extremal positivity bounds in SMEFT: a case study in transversal electroweak gauge-boson scatterings*, JHEP **01** (2021) 095 [[2009.04490](#)].
- [44] Q. Bonnefoy, E. Gendy and C. Grojean, *Positivity bounds on Minimal Flavor Violation*, JHEP **04** (2021) 115 [[2011.12855](#)].
- [45] M. Chala and J. Santiago, *Positivity bounds in the standard model effective field theory beyond tree level*, Phys. Rev. D **105** (2022), no. 11, L111901 [[2110.01624](#)].
- [46] X. Li, K. Mimasu, K. Yamashita, C. Yang, C. Zhang and S.-Y. Zhou, *Moments for positivity: using Drell-Yan data to test positivity bounds and reverse-engineer new physics*, JHEP **10** (2022) 107 [[2204.13121](#)].
- [47] S.-S. Kim, H. M. Lee and K. Yamashita, *Positivity bounds on Higgs-Portal dark matter*, JHEP **06** (2023) 124 [[2302.02879](#)].
- [48] D.-Y. Hong, Z.-H. Wang and S.-Y. Zhou, *Causality bounds on scalar-tensor EFTs*, JHEP **10** (2023) 135 [[2304.01259](#)].
- [49] S.-S. Kim, H. M. Lee and K. Yamashita, *Positivity bounds on Higgs-portal freeze-in dark matter*, JHEP **11** (2023) 119 [[2308.14629](#)].
- [50] Y. Hamada, T. Noumi and G. Shiu, *Weak Gravity Conjecture from Unitarity and Causality*, Phys. Rev. Lett. **123** (2019), no. 5, 051601 [[1810.03637](#)].
- [51] B. Bellazzini, M. Lewandowski and J. Serra, *Positivity of Amplitudes, Weak Gravity Conjecture, and Modified Gravity*, Phys. Rev. Lett. **123** (2019), no. 25, 251103 [[1902.03250](#)].

- [52] G. J. Loges, T. Noumi and G. Shiu, *Duality and Supersymmetry Constraints on the Weak Gravity Conjecture*, JHEP **11** (2020) 008 [[2006.06696](#)].
- [53] L. Alberte, C. de Rham, S. Jaitly and A. J. Tolley, *Positivity Bounds and the Massless Spin-2 Pole*, Phys. Rev. D **102** (2020), no. 12, 125023 [[2007.12667](#)].
- [54] J. Tokuda, K. Aoki and S. Hirano, *Gravitational positivity bounds*, JHEP **11** (2020) 054 [[2007.15009](#)].
- [55] M. Herrero-Valea, R. Santos-Garcia and A. Tokareva, *Massless positivity in graviton exchange*, Phys. Rev. D **104** (2021), no. 8, 085022 [[2011.11652](#)].
- [56] S. Caron-Huot, D. Mazac, L. Rastelli and D. Simmons-Duffin, *Sharp boundaries for the swampland*, JHEP **07** (2021) 110 [[2102.08951](#)].
- [57] S. Caron-Huot, Y.-Z. Li, J. Parra-Martinez and D. Simmons-Duffin, *Causality constraints on corrections to Einstein gravity*, JHEP **05** (2023) 122 [[2201.06602](#)].
- [58] M. Herrero-Valea, A. S. Koshelev and A. Tokareva, *UV graviton scattering and positivity bounds from IR dispersion relations*, Phys. Rev. D **106** (2022), no. 10, 105002 [[2205.13332](#)].
- [59] C. de Rham, S. Jaitly and A. J. Tolley, *Constraints on Regge behavior from IR physics*, Phys. Rev. D **108** (2023), no. 4, 046011 [[2212.04975](#)].
- [60] T. Noumi and J. Tokuda, *Finite energy sum rules for gravitational Regge amplitudes*, JHEP **06** (2023) 032 [[2212.08001](#)].
- [61] K. Aoki, T. Q. Loc, T. Noumi and J. Tokuda, *Is the Standard Model in the Swampland? Consistency Requirements from Gravitational Scattering*, Phys. Rev. Lett. **127** (2021), no. 9, 091602 [[2104.09682](#)].
- [62] T. Noumi and J. Tokuda, *Gravitational positivity bounds on scalar potentials*, Phys. Rev. D **104** (2021), no. 6, 066022 [[2105.01436](#)].
- [63] L. Alberte, C. de Rham, S. Jaitly and A. J. Tolley, *Reverse Bootstrapping: IR Lessons for UV Physics*, Phys. Rev. Lett. **128** (2022), no. 5, 051602 [[2111.09226](#)].
- [64] T. Noumi, S. Sato and J. Tokuda, *Phenomenological motivation for gravitational positivity bounds: A case study of dark sector physics*, Phys. Rev. D **108** (2023), no. 5, 056013 [[2205.12835](#)].
- [65] Y. Hamada, R. Kuramochi, G. J. Loges and S. Nakajima, *On (scalar QED) gravitational positivity bounds*, JHEP **05** (2023) 076 [[2301.01999](#)].
- [66] K. Aoki, T. Noumi, R. Saito, S. Sato, S. Shirai, J. Tokuda and M. Yamazaki, *Gravitational Positivity for Phenomenologists: Dark Gauge Boson in the Swampland*, [2305.10058](#).
- [67] T. Hahn, *Generating Feynman diagrams and amplitudes with FeynArts 3*, Comput. Phys. Commun. **140** (2001) 418–431 [[hep-ph/0012260](#)].
- [68] V. Shtabovenko, R. Mertig and F. Orellana, *FeynCalc 10: Do multiloop integrals dream of computer codes?*, [2312.14089](#).
- [69] H. H. Patel, *Package-X 2.0: A Mathematica package for the analytic calculation of one-loop integrals*, Comput. Phys. Commun. **218** (2017) 66–70 [[1612.00009](#)].
- [70] M. Froissart, *Asymptotic behavior and subtractions in the Mandelstam representation*, Phys. Rev. **123** (1961) 1053–1057.

- [71] A. Martin, *Unitarity and high-energy behavior of scattering amplitudes*, Phys. Rev. **129** (1963) 1432–1436.
- [72] Y. Azimov, *How Robust is the Froissart Bound?*, Phys. Rev. D **84** (2011) 056012 [[1104.5314](#)].
- [73] J. H. Chang, D. E. Kaplan, S. Rajendran, H. Ramani and E. H. Tanin, *Dark Solar Wind*, Phys. Rev. Lett. **129** (2022), no. 21, 211101 [[2205.11527](#)].
- [74] F. Abu-Ajamieh, N. Okada and S. K. Vempati, *Implications of the Weak Gravity Conjecture on Charge, Kinetic Mixing, the Photon Mass, and More*, [2401.10792](#).
- [75] M. A. Buen-Abad, G. Marques-Tavares and M. Schmaltz, *Non-Abelian dark matter and dark radiation*, Phys. Rev. D **92** (2015), no. 2, 023531 [[1505.03542](#)].
- [76] P. Ko and Y. Tang, *Residual Non-Abelian Dark Matter and Dark Radiation*, Phys. Lett. B **768** (2017) 12–17 [[1609.02307](#)].
- [77] J. Ellis, *TikZ-Feynman: Feynman diagrams with TikZ*, Comput. Phys. Commun. **210** (2017) 103–123 [[1601.05437](#)].